Biochemical Pharmacology 80 (2010) 1000–1006

Contents lists available at ScienceDirect

Biochemical Pharmacology

journal homepage: www.elsevier.com/locate/biochempharm

A novel secretagogue increases cardiac contractility by enhancement of L-type Ca^{2+} current

Zhi Su *, Deborah L. Widomski, Xiaoqin Liu, James T. Limberis, Jonathon Green, Gilbert Diaz, Ruth L. Martin, Bryan F. Cox, Gary A. Gintant

Department of Integrative Pharmacology, Global Pharmaceutical Research and Development, Abbott Laboratories, 100 Abbott Park Road, Abbott Park, IL 60064, USA

ARTICLE INFO

Article history:
Received 5 April 2010
Accepted 7 June 2010

Keywords:
L-type Ca^{2+} current
Cardiac myocytes
Rabbit
Inotropy
N′1-(3,3,6,8-tetramethyl-1-oxo-1,2,3,4-tetrahydronaphthalen-2-yliden)-2-cyanoethanohydrazide

ABSTRACT

N′1-(3,3,6,8-tetramethyl-1-oxo-1,2,3,4-tetrahydronaphthalen-2-yliden)-2-cyanoethanohydrazide (TTYC) increases secretion of glucagon-like peptide-1 and intracellular Ca^{2+} concentration in GLUTag cells. The purpose of the present study was to examine if TTYC exerts positive inotropic effects on isolated rabbit ventricular myocytes and in vivo heart in anesthetized rats, and if so to further define the potential mechanism of action. Contractility was assessed in vitro using changes in fractional shortening (FS) of myocyte sarcomere length and in vivo using changes in the velocity of left ventricular pressure. Changes in L-type Ca^{2+} current of ventricular myocytes were evaluated using whole-cell voltage-clamp techniques. TTYC increased FS of myocyte sarcomere length in a concentration-dependent manner. The positive inotropic effect was not abrogated by β-adrenergic blockade (propranolol) or protein kinase A inhibition. TTYC enhanced peak L-type Ca^{2+} current in a voltage-dependent manner (current amplitudes increased by 4.0-fold at -10 mV and 1.5-fold at +10 mV). Voltage-dependence of steady-state activation of L-type Ca^{2+} current was shifted by 15 mV in the negative direction. Inactivation time course of the L-type Ca^{2+} currents at voltages of −10 to 20 mV was significantly slowed by 0.3 μM TTYC. In vivo studies demonstrated that TTYC increased cardiac contractility in a dose-dependent manner. In conclusion, TTYC is a novel L-type Ca^{2+} current activator with positive cardiac inotropic effects. Negative shifting of the voltage-dependence of L-type Ca^{2+} current activation and reduced inactivation are two mechanisms responsible for the enhanced L-type Ca^{2+} current that contribute to the positive inotropic effects.

1. Introduction

Glucagon-like peptide-1 (GLP-1) is an incretin hormone that is mainly produced in the enteroendocrine L cells located in the distal intestine in response to nutrient ingestion [1]. GLP-1 is an attractive novel therapeutic target for diabetes because of its important actions, including stimulation of insulin biosynthesis and secretion, inhibition of glucagon secretion, inhibition of gastric emptying and acid secretion, reduction of food intake, and trophic effect on the beta-cells of the pancreas [1,2].

In an early effort of screening for compounds that can increase GLP-1 secretion, we indentified N′1-(3,3,6,8-tetramethyl-1-oxo-1,2,3,4-tetrahydronaphthalen-2-yliden)-2-cyanoethanohydrazide (TTYC) was able to increase GLP-1 secretion from GLUTag cells (an enteroendocrine cell line) with an EC_{50} value of 3-5 μM (personal communication). Later, it was found that intracellular Ca^{2+} concentration was increased in GLUTag cells exposed to TTYC, suggesting that the secretagogue effect of TTYC on GLP-1 secretion may be associated with the increase of intracellular Ca^{2+} concentration since intracellular calcium is a critical modulator of hormone secretion [3–7]. While the exact mechanism of action for TTYC to increase intracellular Ca^{2+} concentration in GLUTag cells is not fully understood, it was questioned whether TTYC could influence calcium handling and contractility of cardiac myocytes.

The present study was designed to examine potential positive inotropic effects of TTYC in both an in vitro model (acutely isolated rabbit left ventricular myocytes) and an in vivo cardiac model (anesthetized rats), and to understand the potential mechanisms of action. We found that TTYC increased contractile force in isolated left ventricular myocytes (increased fractional shortening) and in vivo rat hearts (increased left ventricular pressure derivative, dP/dt_{50}). We further found that TTYC increased L-type Ca^{2+} channel current in rabbit ventricular myocytes by shifting the voltage-dependence of steady-state activation by 15 mV in the hyperpolarization direction and slowing the time course of inactivation.

* Corresponding author at: Department of Integrative Pharmacology, Abbott Laboratories, R46R-AP9, 100 Abbott Park Road, Abbott Park, IL 60064, USA.
Tel.: +1 847 935 4784, fax: +1 847 938 5286.
E-mail address: zhi.su@abbott.com (Z. Su).

0006-2952/$ – see front matter © 2010 Elsevier Inc. All rights reserved.
doi:10.1016/j.bcp.2010.06.006

2. Methods and materials

2.1. Preparation of ventricular myocytes

Adult rabbit ventricular myocytes were isolated by a modification of a previously reported method [8]. Hearts were removed from rabbits anesthetized with pentobarbital sodium (65 mg/kg, i.v.), were immediately attached to an aortic cannula, and continuous retrograde coronary arterial perfusion at 37 °C was initiated at a perfusion pressure of 60 mmHg. The heart was first perfused with nominally Ca^{2+}-free modified Krebs–Ringer bicarbonate buffer (MKRB) solution for 5 min, immediately followed by 15–25 min of re-circulating perfusion with the MKRB solution containing 1.5 mg/ml collagenase (type II, Worthington Biochemicals, Freehold, NJ), 0.2 mg/ml protease (type XIV, Sigma Chemical, St. Louis, MO), and 50 μM $CaCl_2$. The MKRB solution contained (in mM) 116.7 NaCl, 5 KCl, 1.2 $MgSO_4$, 19 $NaHCO_3$, 1.2 $NaHPO_4$, 15 glucose, and 20 taurine (gassed with 5% CO_2–95% O_2, pH 7.4). The digested heart was then rinsed with MKRB solution containing 50 μM $CaCl_2$ for 3–5 min. The left ventricle was cut into small pieces which were agitated (gentle gassing with 5% CO_2–95% O_2) in the MKRB solution for 5–10 min to disperse myocytes. The myocyte suspension was then incubated for 15–20 min with an equal volume of HEPES-buffered Tyrode's solution containing 1% BSA and 0.2 mM $CaCl_2$. The supernatant was discarded, and the cells resuspended in HEPES-buffered Tyrode's solution containing 1 mM $CaCl_2$. The isolated myocytes were used for studies in HEPES-buffered Tyrode's solution within 6 h after dissociation. The HEPES-buffered Tyrode's solution contained (in mM): 140 NaCl, 5 KCl, 1 $MgCl_2$, 2 $CaCl_2$, 5 glucose, 20 HEPES (pH = 7.4 adjusted with NaOH).

2.2. Measurement of ventricular myocyte contractility

Myocyte contractility was evaluated by measuring changes in fractional shortening of sarcomere length of contracting myocytes. The fractional shortening (FS) was calculated from diastolic and systolic sarcomere length measurements (Fig. 1B) that were continuously monitored and recorded using the IonOptix SarcLen system (IonOptix, Milton, MA, USA) [9]. Left ventricular myocytes were placed in a temperature-controlled (35 °C) superfusion chamber for visualization atop an inverted microscope and electronically stimulated at 1 Hz. Following baseline recordings, myocytes were exposed to ascending concentrations of TTYC (Analogix Inc., Burlington, WI, USA) for a minimum of 5 min for each concentration. In some cases a washout period was performed to evaluate the reversibility of drug effects. FS was calculated using the Ion Optix data analysis software and represents an average of 20 consecutive contractions under each condition. Drug effect on myocyte contractility are expressed as % change relative to the baseline FS. In studies with isolated myocytes, TTYC was prepared as a stock solution in DMSO and then diluted as desired with HEPES-buffered Tyrode's solution. The DMSO concentration in the final perfusate was less than 0.1%. Stock solutions of propranolol and protein kinase A (PKA) inhibitor (fragment 14–22, myristoylated trifluoroacetate salt) were pre-

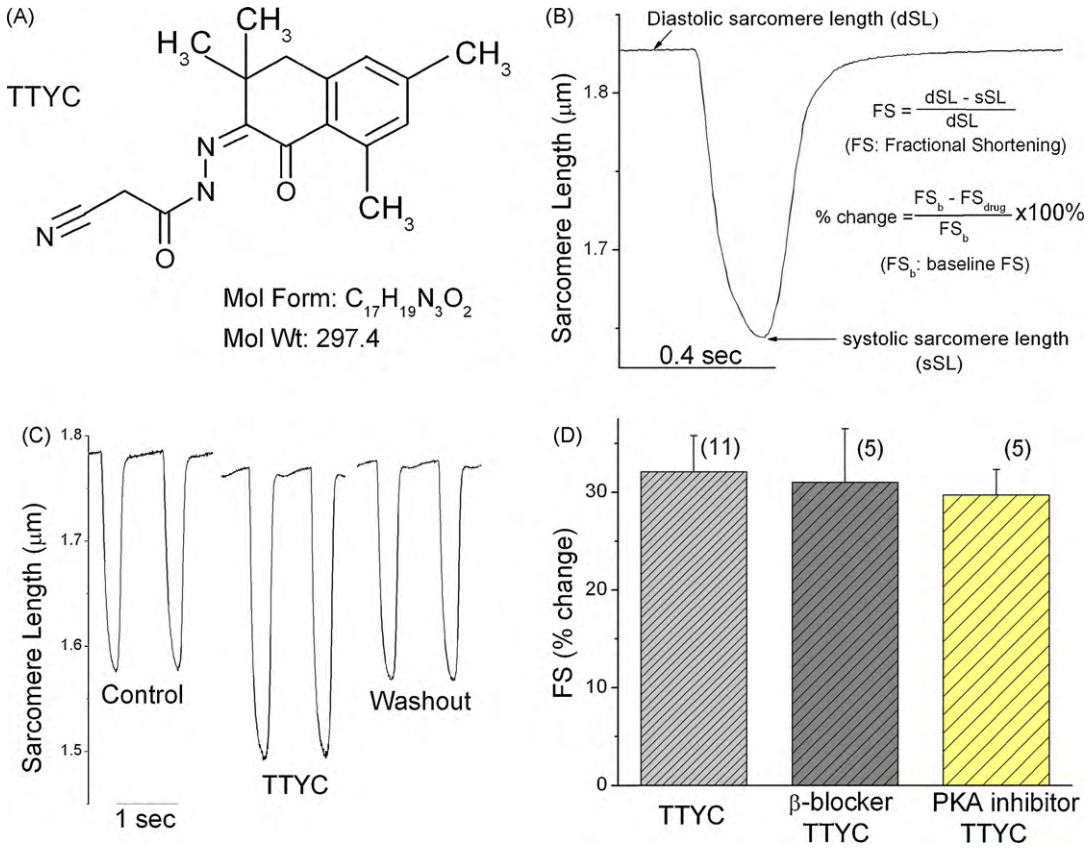

Fig. 1. TTYC increases rabbit myocyte contractility. Panel A, chemical structure for N′1-(3,3,6,8-tetramethyl-1-oxo-1,2,3,4-tetrahydronaphthalen-2-yliden)-2-cyanoethanohydrazide, which is abbreviated (by the authors) as TTYC (Mol Wt. = 297.4; Mol Form: $C_{17}H_{19}N_3O_2$). Panel B, a representative recording of sarcomere length changes during a single contraction of a myocyte. Fractional shortening (FS) and its % change are calculated using the formulas shown in the figure with FS_b being the average fractional shortening (from 20 contractions) during baseline (before drug application) and FS_{drug} the average fractional shortening in the presence of drug. Panel C, representative recordings of sarcomere length (SL) from a myocyte during control period, drug perfusion (0.3 μM TTYC), and washout period. Panel D, TTYC (0.3 μM) increased myocyte contractions in the presence of a β-adrenergic receptor blocker, propranolol (1 μM) or a protein kinase A inhibitor fragment 14–22, myristoylated trifluoroacetate salt (1 μM). Data are expressed as mean ± SEM with "*n*" size shown in the parenthesis.

pared in water. DMSO, Aspartate (K^+ salt), HEPES, Propranolol, and PKA inhibitor were purchased from Sigma–Aldrich (St. Louis, MO). All other chemicals were obtained from Fisher Scientific (Fair Lawn, NJ) unless stated otherwise.

2.3. L-type calcium current recording in ventricular myocytes

L-type Ca^{2+} current was measured at room temperature with a voltage-clamp technique in the absence of external and internal K^+ (replaced by Cs^+) as described previously [8,10]. Myocytes were voltage-clamped with a suction pipette and a voltage-clamp circuit (Multiclamp 700A, Molecular Device, CA). The suction pipettes were made from borosilicate glass capillary tubing and had initial resistances of 1.2–2.2 MΩ when filled with pipette solution containing (in mM): 10 NaCl, 30 tetraethylammonium chloride, 1 $MgCl_2$, 10 EGTA, 5 MgATP, 5 glucose, and 10 HEPES (pH 7.2 with CsOH). CsCl was added to provide a final Cs+ concentration of 110 mM in the pipette solution. The external solution was modified HEPES-buffered Tyrode's solution with KCl replaced by CsCl. Myocytes were held at −80 mV and then clamped to −40 mV for 100 ms (to inactivate Na^+ and T-type Ca^{2+} channel currents) before activating L-type Ca^{2+} channel currents by stepping to test potentials (ranging from −40 to 60 mV in 10 mV increment and 500 ms duration). Currents were filtered at 1–2 kHz and digitized at 2–5 kHz. Software pClamp 9 (Molecular Device, Sunnyvale, CA) was used to generate voltage-clamp protocols and acquire data. Current recordings were digitized with a DigiData 3200 interface (Molecular Device, Sunnyvale, CA), stored on a computer hard disk or a local-area network drive, and analyzed with pClamp 9 (Axon Instruments Inc.) and ORIGIN software (Origin Lab Corporation, Northampton, MA, USA).

2.4. In vivo cardiovascular studies

All studies on experimental animals were conducted under protocols reviewed and approved by the Institutional Animal Care and Use Committee (IACUC) at Abbott Laboratories. Male Sprague-Dawley rats (325–375 g) were anesthetized with Inactin (100 mg/kg, i.p.) and instrumented to record cardiovascular functions as previously described [11]. Briefly, a catheter tipped with a pressure sensor (Millar Instruments, Inc. Houston, TX) was placed in the left ventricle for measurement of left ventricular pressure (LVP) and its derivative (dP/dt_{50}). Mean arterial pressure (MAP) and heart rate were measured through a femoral artery catheter (PE50) connected to a pressure transducer (Transpac II, Abbott Labs, Abbott Park, IL). Via a laparotomy, a pulsed-Doppler cuff type flow probe (Triton Technologies Inc., San Diego, CA) was placed around the upper abdominal aorta just below the diaphragm but above the renal arteries for measurement of peripheral blood flow (PBF, defined as [cardiac output – blood flow to the carotid, coronary, brachiocephalic, and subclavian vessels]). Post hoc, peripheral vascular resistance, PVR, was calculated as MAP/PBF. Femoral vein catheters were used for drug administration and saline infusion (to maintain hydration). Following a stabilization period of at least 1 h after surgery, baseline parameters were recorded at 10-s interval for 30 min. Subsequently, TTYC was infused at 3, 10, and 30 mg/kg/30 min in a polyethylene glycol 400 (PEG 400) vehicle (1 ml/kg/30 min). Primary cardiovascular parameters were recorded using Ponemah data acquisition system (Gould Instrument System Inc., Valley View, OH). Inactin and PEG 400 were purchased from Sigma–Aldrich (St. Louis, MO).

2.5. Statistical analysis

Data were expressed as mean ± SEM (standard error of the mean). Statistical differences were evaluated by one-way ANOVA for repeated measures using SAS software (SAS Institute Inc., Cary, NC, USA) or paired *t*-test where appropriate (Origin Lab Corporation, Northampton, MA, USA). For the in vitro data (isolated myocyte study), comparison was made as control value (prior to drug treatment) vs the steady state value in the presence of TTYC at different test voltages; for the in vivo data (anesthetized rat studies), comparison was made as change from baseline during drug treatment vs change from baseline in vehicle controls. Statistical significance was determined at $P < 0.05$.

3. Results

3.1. Effect of TTYC on isolated rabbit left ventricular myocyte contraction

Representative effects of TTYC on myocyte contractions are shown in Fig. 1.The percent change of fractional shortening (FS) was calculated as illustrated in Fig. 1 B. Following the baseline recording (Fig. 1C), myocytes were exposed to TTYC (0.3 μM) for 5 min. TTYC increased the sarcomere shortening significantly, with mean FS values increased by 16.1 ± 1.2 and 32.1 ± 3.7% at 0.1 ($n = 6$) and 0.3 μM ($n = 11$), respectively. This effect was reversible upon 5-min washout of the TTYC. As shown in Fig. 1C, the resting sarcomere length was also slightly decreased by the addition of TTYC. However, this decrease did not reach statistically significance (1.75 ± 0.02 μm vs 1.71 ± 0.02 μm, $P > 0.05$, $n = 6$). The drug vehicle DMSO had no effect on FS at concentrations up to 0.1% (the highest DMSO concentration in the final drug solution). Bay K-8644, a well-characterized Ca^{2+} channel activator, increased FS by 23.1 ± 2.8% at 10 nM under our experimental conditions (data not shown). To investigate the mechanisms responsible for the positive inotropic effects of TTYC on isolated ventricular myocytes, we examined the TTYC effects on sarcomere shortening in myocytes pretreated with a β-adrenergic receptor blocker (propranolol) or a protein kinase A (PKA) inhibitor (fragment 14–22, myristoylated trifluoroacetate salt). As shown in Fig. 1D, the effect of TTYC (0.3 μM) on fractional shortening was not altered in the presence of propranolol (1 μM) or a PKA inhibitor (1 μM), indicating that the positive inotropic effect of TTYC is not mediated by the β-receptor/cAMP/PKA pathway. The β-adrenergic agonist isoproterenol (10 nM) increased FS by 41.7% under our experimental condition. This positive inotropic effect was completely blocked by 1 μM propranolol (41.7% vs 0.5%) and also prominently suppressed by 1 μM PKA inhibitor (41.7% vs 15.1%).

3.2. Effects of TTYC on L-type Ca^{2+} current of rabbit ventricular myocytes

To further understand the mechanism for the increased fractional shortening of myocytes by TTYC, we examined the effects of TTYC on L-type Ca^{2+} current in rabbit left ventricular myocytes. The L-type Ca^{2+} current was measured using a voltage protocol shown in Fig. 2A. Fig. 2B and C show representative current recordings in the absence (B) and presence (C) of 0.3 μM TTYC. TTYC increased peak L-type Ca^{2+} current in a voltage-dependent manner. For example, current amplitudes were increased by 10-fold at a test potential of −20 mV and 2.1-fold at a test potential of 0 mV. Maximal current was observed at less depolarized potential in the presence (Fig. 2C) than in the absence (Fig. 2B) of TTYC (−10 mV vs +10 mV); this is also demonstrated in Fig. 2E showing the leftward shift of the current–voltage relationship (*I–V* curve) based on the pooled data ($n = 6$). Like the inotropic effects (Fig. 1), effects of TTYC on L-type Ca^{2+} current were also reversible (Fig. 2D).

Fig. 2F shows the effect of TTYC on the voltage-dependence of steady-state activation of the L-type I_{Ca}. To construct the steady-state activation curve, the whole-cell conductance (G) was plotted

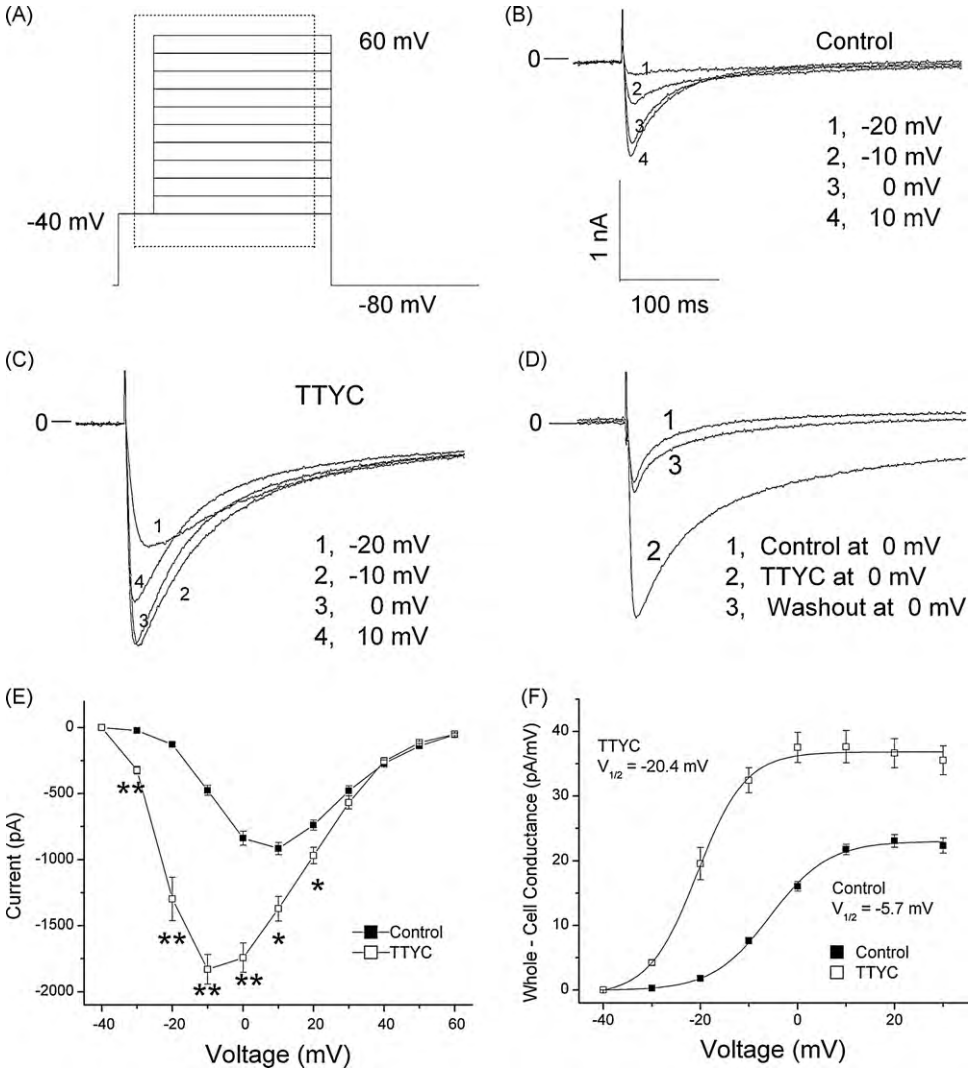

Fig. 2. TTYC increases native cardiac L-type Ca^{2+} Current. Panel A, the voltage protocol used to trigger L-type Ca^{2+} current. Panel B, L-type Ca^{2+} currents recorded using the protocol shown in Panel A, with its peak being at +10 mV under control condition (prior to drug application). Panel C, L-type Ca^{2+} current magnitude increased and peaked at −10 mV after exposure to TTYC (0.3 μM). Currents recorded from the same cell and using the same protocol as in Panel B. Panel D representative currents (recorded at 0 mV from a different cell) showing the reversibility of the TTYC effect on L-type Ca^{2+} currents. Panel E, current–voltage plots in control and the presence of TTYC. Current magnitudes increased in a voltage-dependent manner. Panel F, *G–V* curve (derived from data in Panel E) showing the voltage-dependence of steady-state activation of L-type Ca^{2+} channel. $V_{1/2}$ was shifted to the left by 15 mV in the presence of TTYC. Slope factor was unaltered. Data are expressed as mean ± SEM ($n = 6$). $^{*}P < 0.05$ and $^{**}P < 0.01$ vs vehicle (repeated measures ANOVA).

as a function of test potential (*G–V* curve). *G* value was calculated using an equation: $G = I/(Vt - Vr)$, in which *I* was the measured whole-cell peak current, Vt the test voltage, and Vr the reversal potential. Vr was determined by extrapolation of the current–voltage data (between +10 to +40 mV) shown in Fig. 2E. The *G–V* curve was then fitted with a Boltzmann function to obtain the half maximal activation voltage ($V_{1/2}$) and slope factor. In the absence of TTYC, $V_{1/2}$ was −5.7 ± 1.0 mV with a slope factor of 5.8 ± 0.2 mV ($n = 6$). In the presence of TTYC at 0.3 μM, $V_{1/2}$ was −20.4 ± 1.2 mV with a slope factor of 4.7 ± 0.4 mV ($n = 6$). These results demonstrate that TTYC produces a leftward shift in the voltage-dependence of the L-type Ca^{2+} channel activation.

Voltage- and Ca^{2+}-dependent inactivation of the L-type Ca^{2+} current is an important factor limiting Ca^{2+} influx through the activated Ca^{2+} channels. Fig. 3A and B show that TTYC significantly slows inactivation of L-type Ca^{2+} channel current in the presence of an enhancement of the peak current amplitude. Fast and slow components of the inactivation time course were both slowed (reflected as an increase in the corresponding time constants in Fig. 3C and D) in the voltage range of −10 to 20 mV ($n = 6$ for all voltages tested). It should be noted that TTYC seemed to have greater effect on the slow component of the inactivation time course at +20 mV vs −10 mV. The reason for the apparent voltage-dependent effect is unknown. Data summarized in Table 1 indicate the relative contributions of the slow and fast components to the total inward Ca^{2+} current were also changed by TTYC with the relative amplitude of the slow component increased and the

Table 1
Effects of TTYC on relative contributions of the fast and slow components of L-type Ca^{2+} current inactivation.

Test voltages (mV)	Fast component (%)		Slow component (%)	
	Control	TTYC	Control	TTYC
−10	57.6 ± 0.4	44.7 ± 2.3**	42.3 ± 0.5	55.3 ± 2.3**
0	67.5 ± 1.4	53.8 ± 3.1*	32.5 ± 1.4	46.2 ± 3.1*
10	69.7 ± 2.7	57.5 ± 3.1*	30.3 ± 2.7	42.5 ± 3.1*
20	57.7 ± 4.2	59.9 ± 2.9	42.3 ± 4.2	40.1 ± 2.9

Data were expressed as mean ± SEM ($n = 5$ for each group). $^{*}P < 0.05$ and $^{**}P < 0.01$ vs corresponding components in the control. The relative contribution was calculated as % of total current.

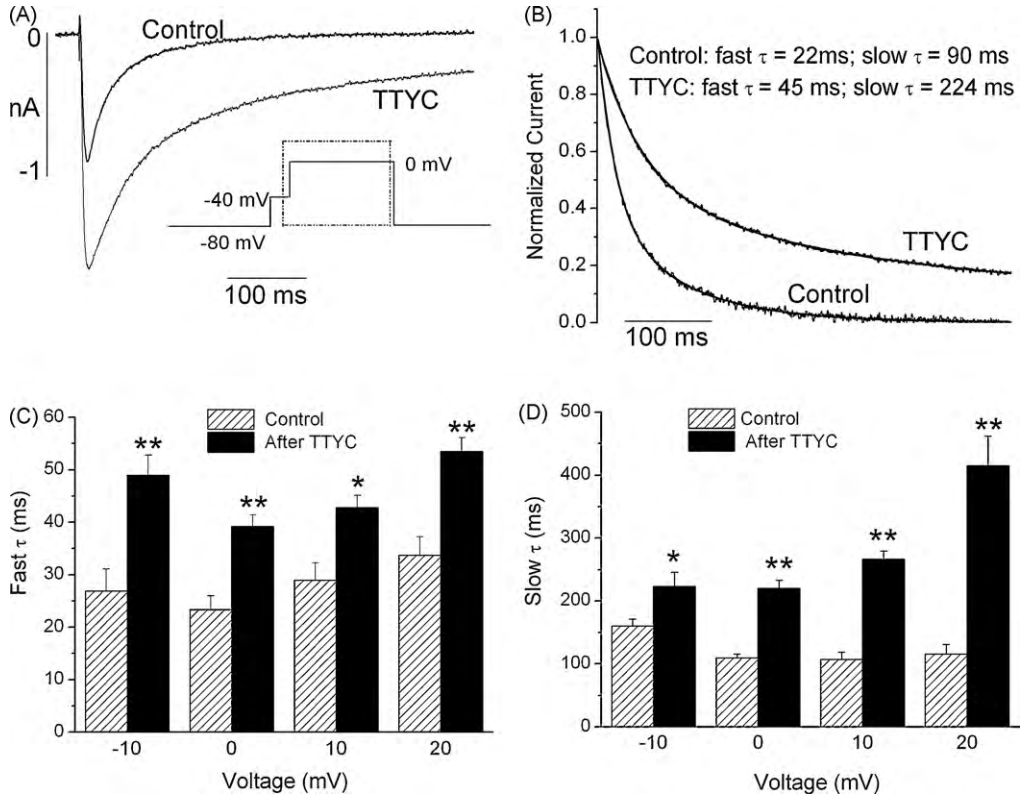

Fig. 3. TTYC slows inactivation kinetics of L-type Ca^{2+} currents. Panel A, example inactivation time course of L-type Ca^{2+} currents in the absence (control) and the presence of TTYC (0.3 μM). Currents were activated using a protocol shown in an inset. Panel B, scaled currents to facilitate comparisons of the inactivation kinetics in the absence and presence of TTYC. The inactivation time course was much slower in the presence of drug. Panels C and D, fast and slow time constants obtained by a double exponential fitting of the data in panel A or B. Fast and slow time constants were significantly increased by TTYC in the voltage range of −10 to 20 mV. Data are expressed as mean ± SEM (n = 6). $^{*}P < 0.05$ and $^{**}P < 0.01$ vs vehicle (repeated measures ANOVA).

relative amplitude of the fast component decreased at voltages of −10, 0, and 10 mV. These results demonstrate that the reduced inactivation by TTYC contributes to the enhanced Ca^{2+} influx during action potential and the enhanced myocyte contractility.

As the amount of Ca^{2+} influx is also affected by channel availability, we therefore examined the effects of TTYC on the voltage-dependence of the steady-state inactivation curve (the availability curve, Fig. 4). There was a slight hyperpolarization shift

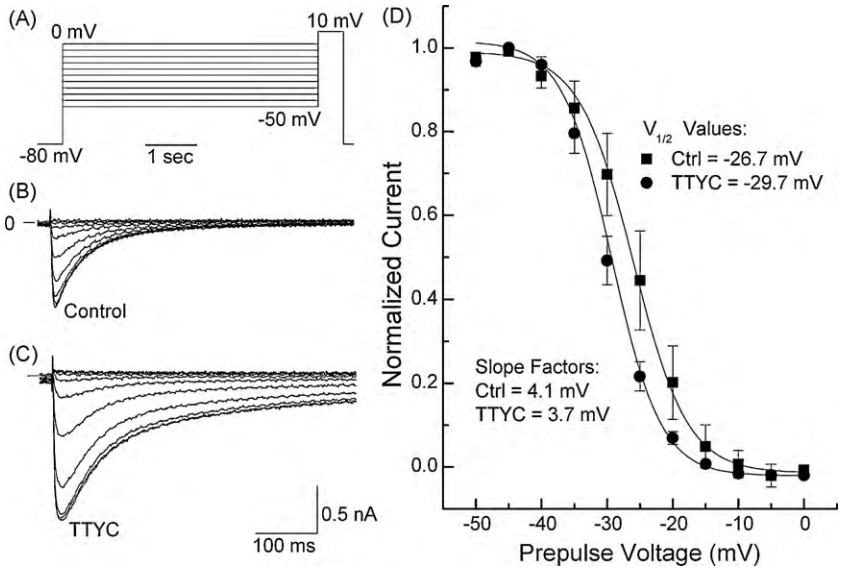

Fig. 4. Effects of TTYC on voltage-dependence of steady-state inactivation of L-type Ca^{2+} channel. Panel A showing the voltage protocol with a test pulse to +10 mV for 500 ms preceded by a 5-s prepulse ranging from −50 to 0 mV (in 5-mV increment) from a holding potential of −80 mV. The voltage protocol was applied every 10 s. Panels B and C, representative currents in control (B) and in the presence of 0.3 μM TTYC (C) were elicited during the test pulse to +10 mV. Panel D, inactivation curves that were fitted with a Boltzmann function yielding $V_{1/2}$ values of −26.7 and −29.7 mV under control and TTYC treatment, respectively. The corresponding slope factors are 4.1 and 3.7 mV, respectively.

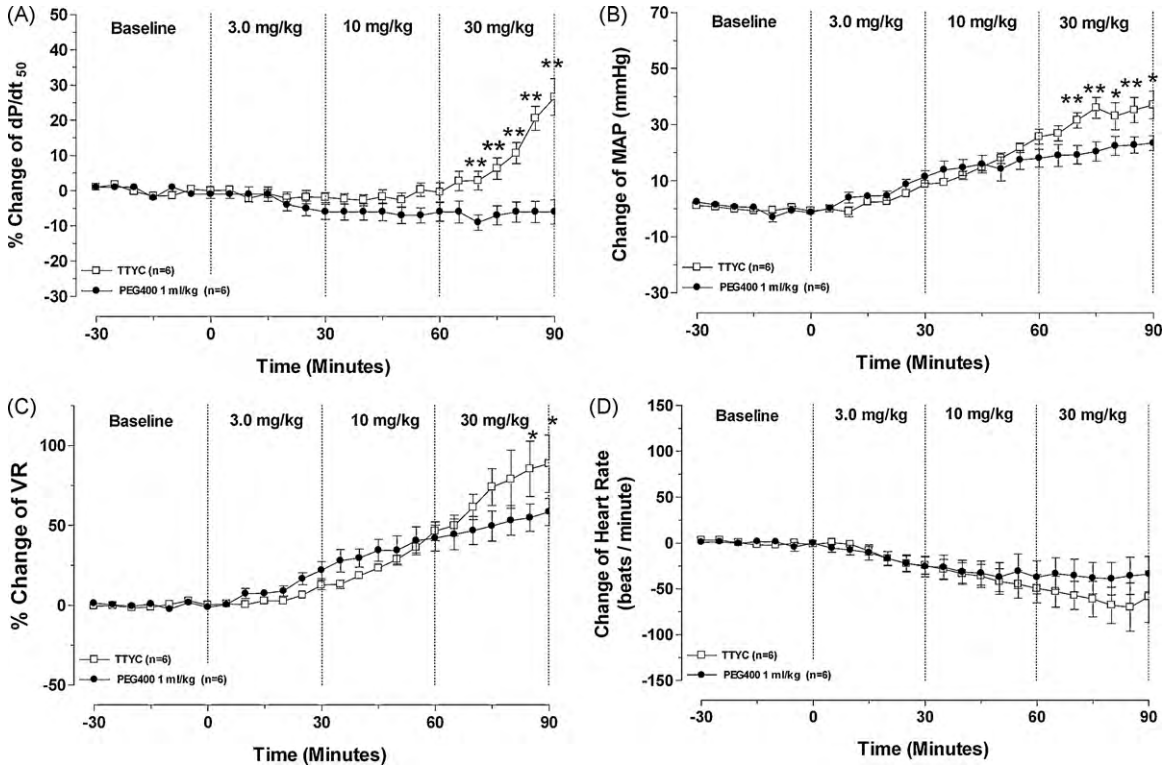

Fig. 5. Cardiovascular effects of TTYC in anesthetized rats. TTYC was administered by i.v. in three ascending doses (3, 10, and 30 mg/kg). Data were expressed as changes from baseline during drug treatment or in vehicle control ($n = 6$/group). Panel A, % change in left ventricular contractility (dP/dt_{50}). Baseline values of dP/dt_{50} were 7645 ± 39 mmHg/s for vehicle and 7456 ± 36 mmHg/s for TTYC. Panel B, change in mean arterial pressure (MAP). Baseline values of MAP were 107 ± 0.7 mmHg for vehicle and 102 ± 0.3 mmHg for TTYC. Panel C, % change in peripheral vascular resistance (VR). Baseline values of VR were 2.5 ± 0.02 mmHg/kHz-shift for vehicle and 2.8 ± 0.02 mmHg/kHz-shift for TTYC. Panel D, change in heart rate. Baseline values of heart rate were 391 ± 1 beats/min for vehicle and 368 ± 1 beats/min for TTYC. For all panels, data were expressed as mean ± SEM. $^{*}P < 0.05$ and $^{**}P < 0.01$ vs vehicle (repeated measures ANOVA). Baseline values for all four parameters were not statistically different between vehicle group and TTYC-treated group.

(3 mV) in the inactivation curve in the presence of TTYC (panel D), which was not statistically significant (−29.7 ± 1.0 mV vs −26.7 ± 1.6 mV, $n = 5$, $P > 0.05$). The slope factor for the inactivation curve was not altered by TTYC (4.1 ± 0.2 mV vs 3.7 ± 0.2 mV, $n = 5$, $P > 0.05$). These results demonstrate that TTYC does not significantly affect the steady-state inactivation curve (i.e., the channel availability for activation) of the L-type Ca^{2+} channel in rabbit ventricular myocytes.

3.3. Cardiovascular effects of TTYC in anesthetized rats

TTYC exhibited multiple hemodynamic effects in the anesthetized rat model. As shown in Fig. 5A, left ventricular dP/dt_{50} was increased in a dose-dependent manner, reaching 32% above vehicle control at the end of the third ascending drug infusion period. Mean arterial pressure and peripheral vascular resistance were also increased during the last infusion with the highest dose at 30 mg/kg (Fig. 5B and C). The heart rate was slightly decreased during the final infusion period (panel D). The decreased heart rate may be reflex-mediated due to the increased mean arterial pressure. Mean plasma concentrations obtained at the end of each infusion period were 2.3 ± 0.3, 8.7 ± 0.7, and 23.5 ± 0.2.0 μM ($n = 6$), respectively. Overall, the in vivo cardiovascular effects of TTYC are consistent with its action as an L-type calcium channel activator.

4. Discussion

The present study demonstrated for the first time a positive inotropic effect for TTYC in both in vitro and in vivo cardiac models consistent with its effects on L-type Ca^{2+} current. TTYC increased L-type Ca^{2+} current amplitudes in a voltage-dependent manner. For example, current amplitudes were increased by 10-fold at −20 mV and 2.1-fold at 0 mV. This effect is consistent with a hyperpolarization shift (by 15 mV) of the voltage-dependence of the steady-state activation for L-type Ca^{2+} channels in rabbit cardiac myocytes in the presence of TTYC (Fig. 2). TTYC also significantly slowed the inactivation kinetics of the L-type Ca^{2+} channel (Fig. 3), which would be one of the major effects leading to the increased Ca^{2+} current or influx during the cardiac action potential. TTYC did not significantly affect the voltage-dependence of steady-state inactivation curve for L-type Ca^{2+} channels, indicating that the channel availability for activation is not changed by TTYC. Thus, at least two biophysical mechanisms contribute towards the enhanced L-type Ca^{2+} current: negative shift of the voltage-dependent activation and the reduced inactivation.

The positive inotropic effect of TTYC was not altered in the presence of propranolol or a PKA inhibitor, indicating that the β-receptor/cAMP/PKA pathway-mediated modulation of L-type current was (at least) not the major mechanism responsible for the enhanced L-type Ca^{2+} current and the positive inotropic effect of TTYC. Although the TTYC-mediated enhancement of L-type Ca^{2+} current is consistent with its positive inotropic effect on isolated myocytes, it should be noted that cardiac inotropy can be modulated by multiple mechanisms such as myofilament sensitivity to Ca^{2+}, phosphodiesterase activity, Ca^{2+} current and Na/Ca exchange, sarcoplasmic reticulum Ca^{2+} uptake and release [12–14]. Therefore, results presented in this study should not exclude the aforementioned mechanisms that might contribute to the enhanced cardiac contractility observed with TTYC.

Consistent with the positive inotropic effects on isolated ventricular myocytes, left ventricular contractility was also increased by TTYC in anesthetized rats in a dose-dependent

manner as evidenced by the increases in left ventricular dP/dt_{50} (Fig. 5). It is likely the in vivo cardiac inotropic effect is also mediated (at least partially) by the enhanced L-type Ca^{2+} current in myocytes although other mechanisms cannot be excluded. It should also be noted that significant increase in left ventricular contractility occurred at relatively high plasma concentrations (32% increase at 23.5 μM) in contrast to a significant increase of contractility in vitro (32% increase at 0.3 μM). The potency shift for TTYC from in vitro to in vivo studies may be due to plasma protein binding in vivo. It is also possible that the species difference (rabbit vs rat) could contribute to the potency shift between in vitro and in vivo results. In the in vivo study (Fig. 5), we also observed an increase in peripheral vascular resistance during the final infusion period, suggestive of L-type Ca^{2+} channel activation in vascular smooth muscle. The increase in MAP was likely caused by the concomitant increase in peripheral vascular resistance and cardiac contractility. Theoretically, L-type Ca^{2+} current enhancement would increase heart rate [15]. However, the heart rate in TTYC-treated rats was slightly decreased during the final infusion period. The decreased heart rate may be reflex-mediated due to the increased mean arterial pressure.

L-type Ca^{2+} channel is expressed in cardiac myocytes (Ca_V 1.2) and endocrine tissues (Ca_V 1.2 and Ca_V 1.3) [1,16]. Therefore, the effect of TTYC on L-type Ca^{2+} current may explain the increase in intracellular Ca^{2+} concentration observed in GLUTag cells. This is consistent with previous findings that enhanced Ca^{2+} influx through L-type Ca^{2+} channels is responsible for GLP-1 release from intestinal L-cells or GLUTag cells in response to a range of nutrients [6,7]. Similar to the mechanisms of action for the positive inotropic effects of TTYC, however, it is also true that increase of intracellular Ca^{2+} concentration through the enhanced L-type Ca^{2+} current should not exclude other additional mechanisms by which TTYC might increase GLP-1 secretion from GLUTag cells.

Results in the present study indicate secretagogues through L-type Ca^{2+} channel activation (like TTYC) could have hemodynamic effects as shown by the significant increase in cardiac contractility and elevation of arterial blood pressure. Therefore, in the discovery of novel secretagogues targeting L-type Ca^{2+} channels, highly subtype- or tissue-selective L-type Ca^{2+} channel activators are required to avoid potential cardiovascular side effects. Actually, TTYC exhibited little tissue selectivity between secretary cells and cardiac myocytes based on the preliminary EC_{50} value of 3–5 μM for GLP-1 secretion and significant increases in cardiac contractility (32% increase at 0.3 μM in vitro and 32% increase at 23.5 μM in vivo), indicating that TTYC has an unacceptable safety margin in terms of cardiovascular effects. L-type Ca^{2+} channel activation could also be potentially proarrhythmic due to prolongation of action potential duration and intracellular Ca^{2+} overloading in the myocardium [17]. It has been reported that enhanced L-type Ca^{2+} channel activity may induce early afterdepolarizations (EADs) and the polymorphic tachycardiac Torsade de pointes [17–19].

In conclusion, TTYC is a novel secretagogue that activates L-type Ca^{2+} channel and exerts positive cardiac inotropic effects. Negative shifting of the voltage-dependence of the L-type Ca^{2+} channel activation and the reduced inactivation are two mechanisms responsible for the enhanced L-type Ca^{2+} current. These findings also highlight potential cardiovascular safety issues that may arise with some secretagogues.

References

[1] Gautier JF, Choukem SP, Girard J. Physiology of incretine (GIP and GLP-1) and abnormalities in type 2 diabetes. Diabetes Metab 2008;34(Suppl. 2): S65–72.

[2] Vilsboll T, Holst JJ, Knop FK. The spectrum of antidiabetic actions of GLP-1 in patients with diabetes. Best Pract Res Clin Endocrinol Metab 2009;23: 453–62.

[3] Schulla V, Renstrom E, Feil R, Feil S, Franklin I, Gjinovci A, et al. Impaired insulin secretion and glucose tolerance in β cell-selective Ca_V Ca^{2+} channel null mice. EMBO J 2003;22:3844–54.

[4] Rutter GA, Tsuboi T, Ravier MA. Ca^{2+} microdomains and the control of insulin secretion. Cell Calcium 2006;40:539–51.

[5] Rose T, Efendic S, Rupnik M. Ca^{2+}-secretion coupling is impaired in diabetic Goto Kakizaki rats. J Gen Physiol 2007;129:493–508.

[6] Reimann F, Maziarz M, Flock G, Habib AM, Drucker DJ, Gribble FM. Characterization and functional role of voltage gated cation conductances in the glucagons-like peptide-1 secreting GLUTag cell line. J Physiol 2005;563:161–75.

[7] Reimann F, Ward PS, Gribble FM. Signaling mechanisms underlying the release of glucagons-like peptide 1. Diabetes 2006;55:S78–85.

[8] Yao A, Su Z, Nonaka A, Zubair I, Spitzer KW, Bridge HB, et al. Abnormal myocyte Ca^{2+} homeostasis in rabbits with pacing-induced heart failure. Am J Physiol Heart Circ Physiol 1998;274:H1441–8.

[9] Nishimura S, Yasuda S, Katoh M, Yamada KP, Yamashita H, Saeki Y, et al. Single cell mechanics of rat cardiomyocytes under isometric, unloaded, and physiologically loaded conditions. Am J Physiol Heart Circ Physiol 2004;287:H196–202.

[10] Su Z, Sheets M, Ishida H, Li F, Barry WH. Saxitoxin blocks L-type I_{Ca}. J Pharmacol Exp Ther 2004;308:324–9.

[11] Segreti JA, Marsh KC, Polakowski JS, Fryer RM. Evoked changes in cardiovascular function in rats by infusion of Levosimendan, OR-1896, OR-1855, Dobutamine, and Milrinone: comparative effects on peripheral resistance, cardiac output, dP/dt, pulse rate, and blood pressure. J Pharmacol Exp Ther 2008;325:331–40.

[12] Bers DM. Excitation-contraction coupling and cardiac contractile force. Dordrecht: Kluwer Academic Publishers; 2001.

[13] Barry WH, Bridge JHB. Intracellular calcium homeostasis in cardiac myocytes. Circulation 1993;87:1806–15.

[14] Su Z, Barry WH. Isolated myocyte mechanics and calcium transients. In: Hoit BD, Walsh RA, editors. Cardiovascular physiology in the genetically engineered mouse. Dordrecht: Kluwer Academic Publishers; 2001. p. 71–89.

[15] Schram G, Pourrier M, Melnyk P, Nattel S. Differential distribution of cardiac ion channel expression as a basis for regional specialization in electrical function. Circ Res 2002;90:939–50.

[16] Eertel EA, Campbell KP, Harpold MM, Hofmann F, Mori Y, Perez-Reyers E. Nomenclature of voltage-gated calcium channels. Neuron 2000;25:533–5.

[17] Tweeddie D, Harding SE, MacLeod KT. Sarcoplasmic reticulum Ca content, sarcolemmal Ca influx and the genesis of arrhythmias in isolated guinea-pig cardiomyocytes. J Mol Cell Cardiol 2000;32:261–72.

[18] January CT, Riddle JM, Salata JJ. A model for early afterdepolarizations: induction with the Ca^{2+} channel agonist Bay K 8644. Circ Res 1988; 62:563–71.

[19] Mazur A, Roden DM, Anderson ME. Systemic administration of calmodulin antagonist W-7 or protein kinase A inhibitor H-8 prevents Torsade de Pointes in rabbits. Circulation 1999;100:2437–42.